International Journal of Fatigue 93 (2016) 363–371

Contents lists available at ScienceDirect

International Journal of Fatigue

journal homepage: www.elsevier.com/locate/ijfatigue

The potential of spinodal ferrite decomposition for increasing the very high cycle fatigue strength of duplex stainless steel

U. Krupp [a,d,*], M. Söker [a], A. Giertler [a], B. Dönges [b], H.-J. Christ [b], K. Wackermann [c], T. Boll [d], M. Thuvander [d], M.C. Marinelli [e]

[a] Institute of Materials Design and Structural Integrity, Faculty of Engineering and Computer Science, University of Applied Sciences Osnabrück, 49009 Osnabrück, Germany
[b] Institut für Werkstofftechnik, Universität Siegen, 57068 Siegen, Germany
[c] Fraunhofer Institute for Mechanics of Materials IWM, Freiburg, Germany
[d] Division of Materials Microstructure, Department of Physics, Chalmers University of Technology, 41296 Göteborg, Sweden
[e] Instituto de Física Rosario – Consejo Nacional de Investigaciones Científicas y Técnicas (CONICET), Universidad Nacional de Rosario, 2000 Rosario, Argentina

ARTICLE INFO

Article history:
Received 11 February 2016
Received in revised form 13 May 2016
Accepted 14 May 2016
Available online 14 May 2016

Keywords:
Duplex stainless steel
Spinodal decomposition
Very high cycle fatigue
Atom probe tomography

ABSTRACT

Duplex stainless steels (DSS) have become candidate materials for structural applications, where conventional austenitic stainless steels fail due to very high cycle fatigue (VHCF) in combination with corrosive attack. It seems that DSS exhibit a fatigue limit, which can be attributed to the two-phase austenitic–ferritic microstructure. Ultrasonic VHCF testing revealed that the phase boundaries are efficient obstacles for the transmission of slip bands and microstructural fatigue cracks up to 10^9 cycles and even beyond. The barrier strength is determined by the misorientation relationship between neighbouring grains but also by the strength of the individual phases. By thermal treatment at 475 °C, spinodal decomposition of the ferrite phase results in the formation of Cr-rich α′ precipitates. While during static loading these precipitates give rise to a loss in ductility (475 °C embrittlement), it was shown that the HCF strength can be increased and that there is also a tendency towards a beneficial effect on the VHCF behaviour. A more detailed analysis of the local plasticity sites by means of atom probe tomography (APT) revealed a dissolution of the α′ precipitates within operated slip bands. The dissolution might be an indication for a local softening mechanism that limits the VHCF strengthening effect of spinodal decomposition.

1. Introduction

Increasing use of renewable energies, e.g. by wind power plants, biogas plants and solar-thermic power plants, as well as hazard conditions in chemical reactors, has led to a substantial demand for new corrosion-resistant high strength materials, which are weldable, machinable and available on the market for reasonable costs. Duplex stainless steels (DSS) are promising materials for structural applications involving fatigue loading in corrosive environments up to very high numbers of cycles (very high cycle fatigue, VHCF) [1,2]. It has been shown that the VHCF strength of DSS depends strongly on the barrier efficiency of the phase boundaries. VHCF damage sets in by accumulation of cyclic plasticity within grains of the softer fcc austenite phase that are oriented for easy slip, i.e., grains exhibiting a high resolved shear stress acting on the slip systems [3]. Accumulation of cyclic plasticity manifests itself by an increased density in slip bands, the spread of which is blocked by the phase boundaries towards adjacent ferrite grains. It has been observed that exceeding a certain degree of plasticity in the fcc austenite grains leads to slip transmission into the neighbouring bcc ferrite grains and eventually, to initiation of fatigue cracks. Therefore, VHCF life of duplex stainless steels is infinite (fatigue limit) once the blocking effect of phase boundaries is sufficient to withstand the transmission of slip and microstructurally short cracks, respectively (cf. [4]). The blocking efficiency is determined by the degree of coplanarity between the slip systems of the neighbouring grains. Quantification of the blocking efficiency has been the subject of numerous research activities. According to Zhai et al. [5] and Marx et al. [6], the major contribution is due to the twist misorientation ξ between neighbouring slip systems, since accommodation of an additional grain boundary plane is required to shift the slip band from one grain to another, as shown schematically in Fig. 1. In the case of DSS, the Kurdjumov–Sachs relationship (KS) between austenite and ferrite grains is fulfilled to a large extent and can be implemented to analyse

* Corresponding author at: Institute of Materials Design and Structural Integrity, Faculty of Engineering and Computer Science, University of Applied Sciences Osnabrück, 49009 Osnabrück, Germany.
E-mail address: u.krupp@hs-osnabrueck.de (U. Krupp).

http://dx.doi.org/10.1016/j.ijfatigue.2016.05.012
0142-1123/

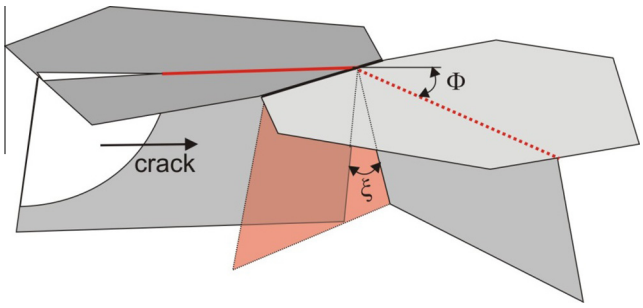

Fig. 1. Schematic representation of the geometrical concept for the blocking effect of grain and phase boundaries. The main contribution is due to the twist angle ξ, rather than to the tilt angle Φ.

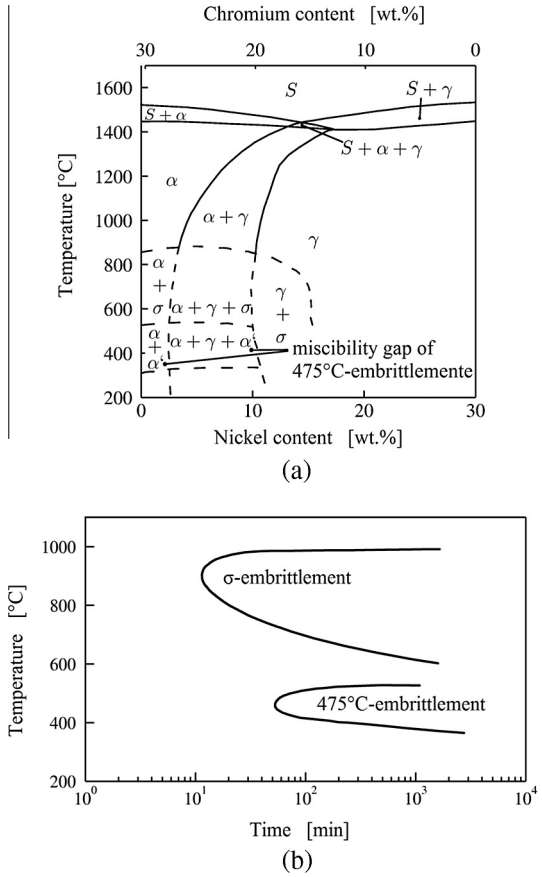

Fig. 2. (a) Quasi-binary section of the Fe–Cr–Ni phase diagram (70 wt.% Fe) showing the regime of spinodal decomposition, and (b) time temperature transition (TTT) diagram of the DSS 1.4462 (as used in the present study) showing the regime of σ phase formation and 475° embrittlement (according to [12]).

short fatigue crack propagation [7]. This geometrical relationship involving the spatial arrangement of grain and phase boundary planes and the orientation of the operated slip systems has been used in software packages, e.g., ARGE to describe the blocking efficiency [8] and a mechanism-based short crack model based on the boundary element method, as it is described e.g. in [9].

Furthermore, the fatigue damage behaviour of DSS depends on the strength of the individual phases austenite and ferrite. The austenite phase can be strengthened by increasing the nitrogen concentration, resulting in a substantial increase in fatigue strength of the so-called super duplex steel (cf. [2,10]). The ferrite phase is susceptible to σ-phase formation at elevated temperatures

Table 1
Chemical composition of the duplex steel 1.4462 (SAE2205) (wt.%).

Fe	C	Cr	Ni	Mo	Mn	N	P	S
bal.	0.02	21.9	5.6	3.1	1.8	0.19	0.023	0.002

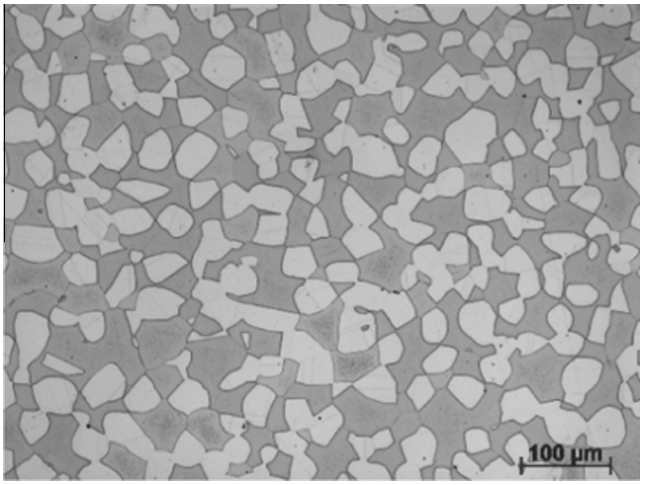

Fig. 3. Micrograph of duplex stainless steel (DSS) 1.4462, showing the fcc austenite phase as light grey grains within the dark grey bcc ferrite matrix.

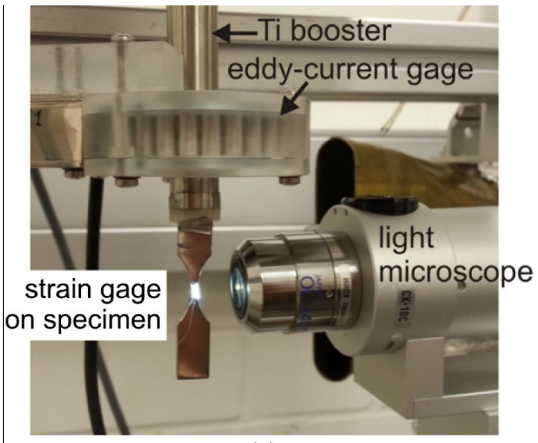

Fig. 4. Ultrasonic fatigue testing: (a) in combination with a light microscope (the eddy current gage is marked by an arrow), (b) for *in-situ* VHCF damage observation in the SEM (cf. [17]).

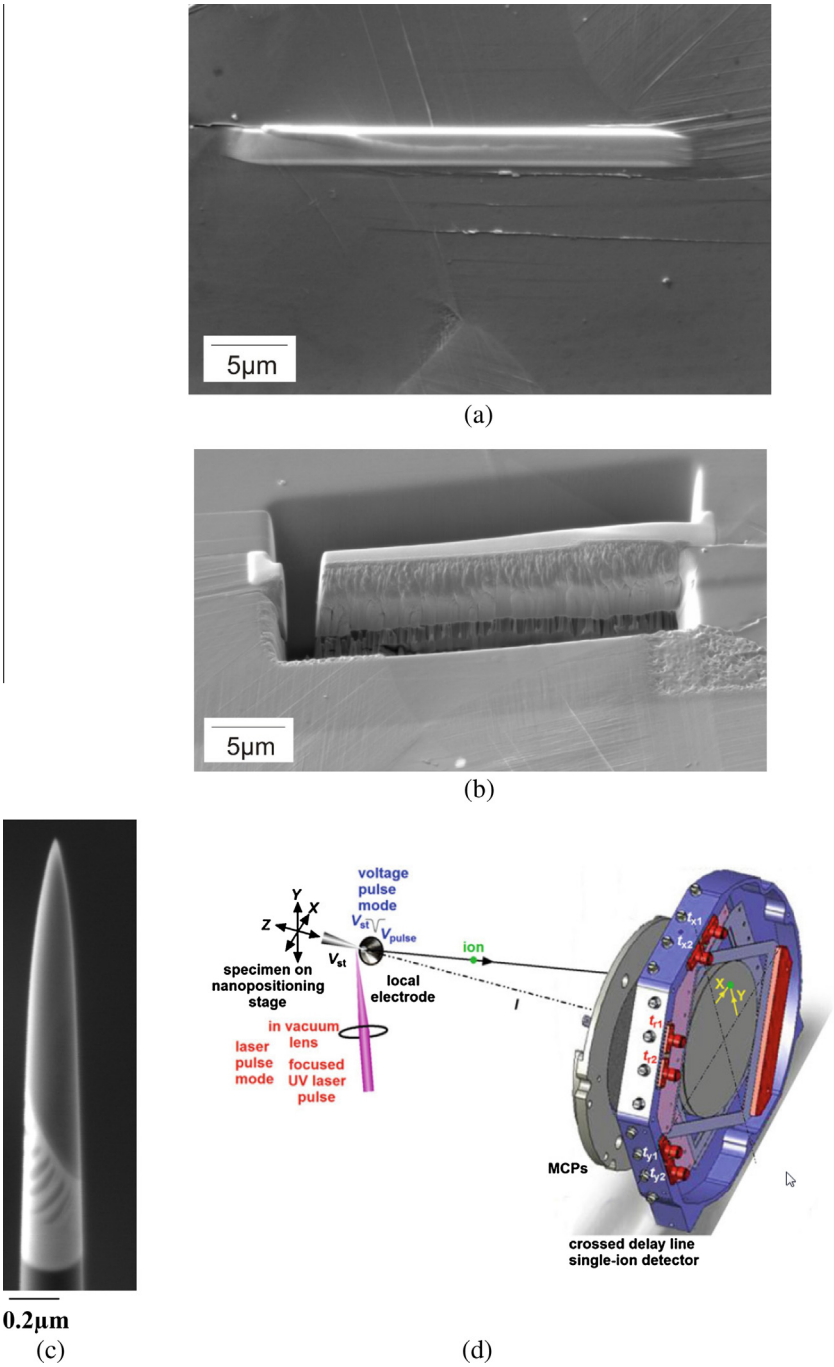

Fig. 5. Preparation of DSS tips for atom probe tomography (APT): (a) stabilization of the slip band area by Pt deposition, (b) FIB milling of a lamella, (c) fully prepared tip of plastically deformed ferrite for APT, (d) schematic representation of local electrode APT [18].

(600–1000 °C), and the so-called "475 °C embrittlement" leading to a substantial increase in hardness [11]. The mechanism of "475 °C embrittlement" can be understood as spontaneous spinodal decomposition of the ferrite, in Cr-rich bcc α' clusters within the Fe-rich α matrix by uphill diffusion, which is driven by a free energy decrease resulting from a spontaneous decomposition within the miscibility gap of the Fe Cr system (cf. Fig. 2) [11,12].

Several aspects of hardening due to spinodal decomposition of ferrite are discussed. Generally, the Cr-rich α' zones show a lattice mismatch with respect to the parent bcc α matrix. They cause a localization of plastic slip and they are sheared by dislocations (cf. [1,11]). Depending on the degree of ferrite embrittlement, a pronounced drop in toughness can be observed (cf. [11,13]) since at high α' content ferrite tends to cleavage fracture along {100} planes. Shear accumulation during fatigue loading seems to accommodate the decomposition leading to the disappearance of the modulations in the Cr concentration, as it was shown by [14,15]. From thermomechanical fatigue (TMF) experiments on duplex steel in the temperature range between 300 °C and 600 °C it was concluded that the 475° embrittlement is reversible, i.e., the formed α' precipitates can be dissolved quite rapidly when the temperature exceeds 500 °C [16].

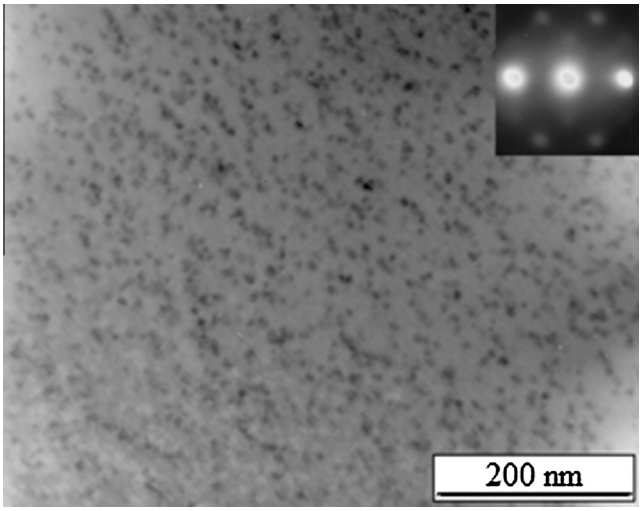

Fig. 6. TEM micrograph of DSS in the fully embrittled condition (100 h annealing at 475 °C).

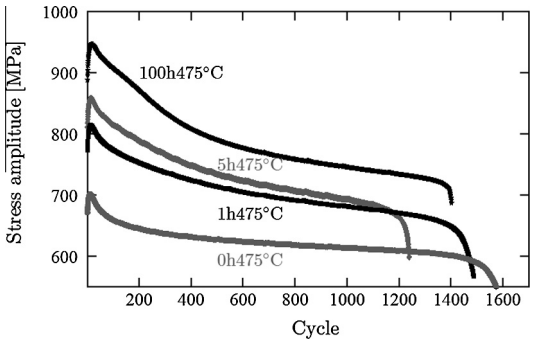

Fig. 7. Cyclic deformation curves (strain control $\Delta\varepsilon/2 = 1\%$ and $R_\varepsilon = -1$) on four differently embrittled conditions.

Today, the question remains open, whether 475 °C embrittlement generally causes a deterioration of the mechanical properties of DSS and therefore limits their application to rather low temperatures or if a tailored thermal embrittlement allows the adaptation of the barrier efficiency of austenite ferrite phase boundaries, leading to an increase in VHCF strength. It is subject of the present paper to compare the fatigue behaviour of embrittled and non-embrittled DSS specimens taking into account interactions between the α′ zones and local plastic slip.

2. Experimental

Prior to cyclic loading, specimens of the duplex stainless steel DSS 1.4462 (German designation, corresponds to SAE2205) with a chemical composition as given in Table 1, underwent a heat treatment consisting of (i) a grain coarsening treatment at 1250 °C (4 h) followed by slow cooling in air to 1050 °C and final water quench, and (ii) an embrittlement treatment at 475 °C for various times (fully embrittled was considered after 100 h annealing).

Fig. 3 shows the DSS two-phase microstructure with about 50% fcc austenite grains (mean grain size of 46 μm, Vickers hardness 260HV) precipitated within the 50% parent bcc ferrite phase (mean grain size of 33 μm, Vickers hardness of 280HV and 465HV in the non-embrittled in the fully embrittled condition, respectively).

Cylindrical fatigue specimens were machined and electropolished to analyse surface fatigue damage by means of scanning electron microscopy (SEM) in combination with automated electron back-scatter diffraction. Cyclic loading was carried out using a MTS type 810 servohydraulic testing machine (push pull LCF testing, strain control, fully reversed cycling, $R = -1$), a conventional rotating bending machine (type Schenk, HCF testing) and ultrasonic testing systems tailor-made by BOKU Vienna for VHCF testing at 20 kHz and a stress ratio of $R = -1$. In the latter case, a constant stress during the test is maintained, by first using a strain gage attached to the specimen surface. Since this strain gage fails after a number of cycles, the system operates by displacement control using an eddy current gage placed around the Ti booster (cf. Fig. 4a). To avoid specimen heating, the system operates in a pulse-pause mode. For *in-situ* VHCF damage tracking at the surface, the testing system can be used (i) in combination with a light microscope (Fig. 1a) and (ii) within the testing chamber of a SEM (Zeiss Auriga) (Fig. 1b, cf. [17]).

Some of the fatigue tests were periodically interrupted to track fatigue damage. In general, fatigue tests were terminated when 10^9 load cycles were reached (run-out specimens). Three of the fully embrittled run-out specimens were used for atom probe tomography (APT) in an Imago LEAP 3000X HR to reveal changes in the α′-cluster distribution of the plastically deformed ferrite grains. For this purpose, the region of interest (slip bands) was covered with Pt deposition within a FEI Versa FIB SEM to stabilize the slip bands for the ongoing tip preparation (see Fig. 5a). Then, a lamella containing the slip bands was cut out by focussed-ion-beam milling (FIB, Fig. 5b) and extracted with an Omniprobe micromanipulator. Segments of the lamella were placed on the small cylindrical posts o fa Cameca Si flattop microtip coupon by FIB-cutting and Pt-deposition. As a final step, annular FIB milling was applied to produce small needle-shaped tips (Fig. 5c). From these tips atoms are field evaporated within a standing high electric field by an additional voltage or laser pulse and detected by a 2D delay line detector; according to the schematic representation in Fig. 5d. The time of flight of the ions allows the identification of the respective elements and the sequence and detected position the reconstruction of the position in 3D. For this purpose, the Cameca IVAS software was utilized. For details about the APT technique refer to [18]. The presented measurements were conducted at 60 K with laser pulsing of the green LEAP 3000X HR laser at 100 kHz and pulse energies of 200 pJ.

3. Results

Spinodal decomposition of the ferrite (475° embrittlement) leads to the formation of Cr-rich clusters. In the transmission electron microscope (TEM) they appear as homogeneously distributed dark precipitates of approximately 10 nm diameter. This is shown in the micrograph in Fig. 6. Full embrittlement was shown to be achieved in DSS after about 1 h of thermal treatment at 475 °C by Charpy testing [19], revealing a drop in impact fracture toughness from 200 J in the non-embrittled condition to less than 20 J in the fully embrittled condition.

During LCF testing of DSS in different embrittlement stages, generally cyclic strengthening followed by cyclic softening can be observed. However, the cyclic deformation curves in Fig. 7 reveal a pronounced softening of embrittled specimens. According to Park et al. [14] and Herenú et al. [15], this can be attributed to a disappearance of spinodal decomposition, i.e., local dissolution of the α′ phase. In [15] this was confirmed by analytic TEM using EDS line analysis across plastically active areas within embrittled DSS, where a disappearance of the Cr modulation (due to α′ precipitates) was correlated with the presence of slip bands (cf. Fig. 13).

According to a high number of fatigue experiments carried out on DSS in the non-embrittled and fully embrittled steel, it seems

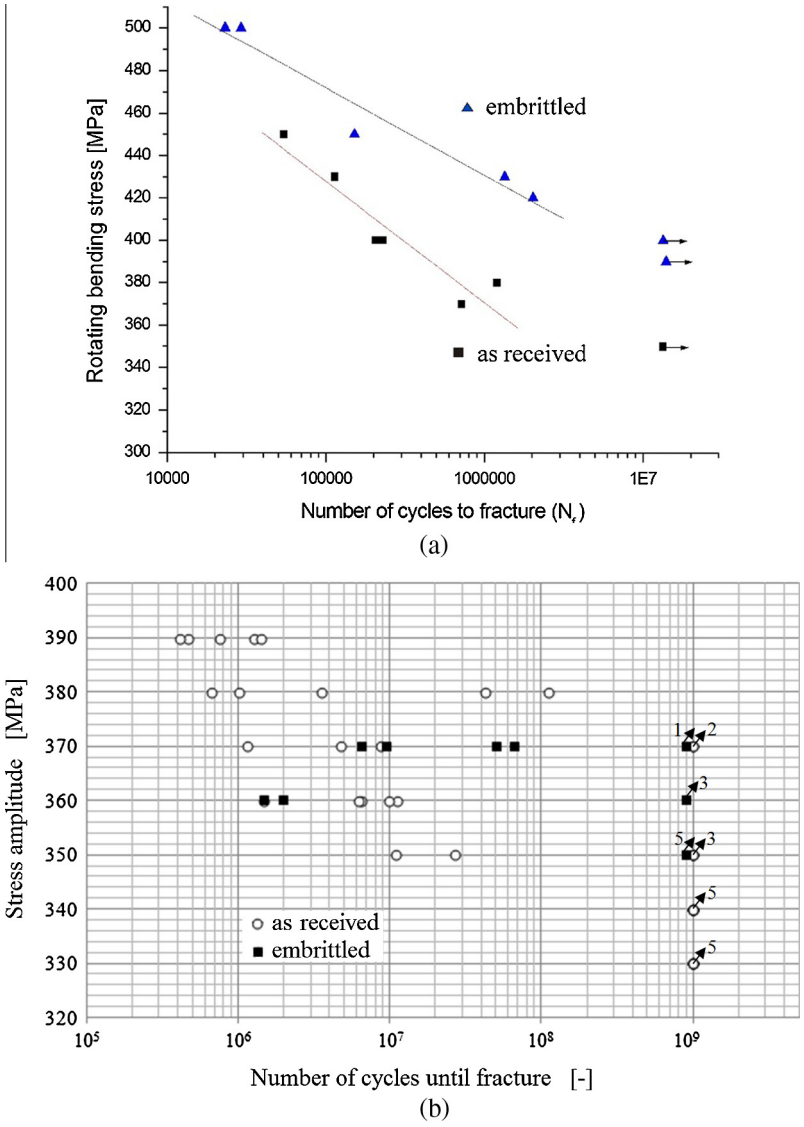

Fig. 8. S–N-Wöhler diagram in the as-received and in the fully embrittled condition (100 h anneal at 475 °C) obtained by means of (a) rotating bending tests and (b) obtained by means of ultrasonic fatigue testing at 20 kHz.

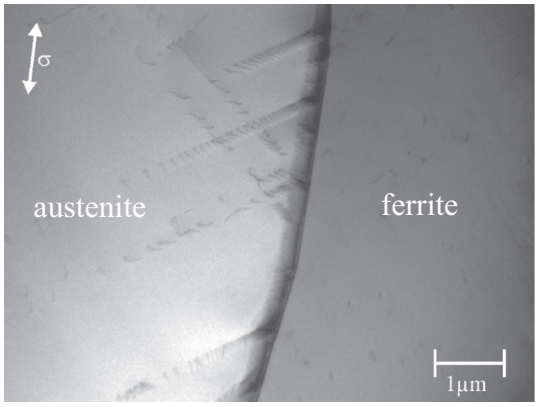

Fig. 9. Dislocation pile-ups at an austenite (left) ferrite (right) phase boundary, zone axes: [1 2 2] (austenite) and [1 1 1] (ferrite) ($\Delta\sigma/2$ = 300 MPa, run-out).

that due to the two-phase microstructure DSS exhibits a real fatigue limit. Specimens that survive 10^7 cycles can be considered as run-out specimens (here: 10^9 cycles). The fatigue limit has been estimated as σ_{FL} = 360 MPa. A selection of S/N results is presented in Fig. 8, as obtained from rotating bending tests (Fig. 8a, cf. [20]) and ultrasonic push–pull loading (Fig. 8b).

In the HCF and the VHCF regime fatigue, damage is almost always initiated at the surface by slip band formation within the softer austenite phase, followed by crack nucleation preferentially at intersections between slip bands and phase boundaries (cf. [20]). Only in the case of very few specimens, internal failure at a non-metallic inclusion (Al_2O_3) was observed leading to the characteristic fish-eye formation [21].

From the rotating-bending tests, it is obvious that the fatigue strength is increased for fully-embrittled specimens in the transition regime from HCF to VHCF ($N_F = 10^5$–10^7 cycles). In the case of ultrasonic testing ranging up to 10^9 cycles only a tendency towards an increase in VHCF strength was observed. Due to a substantial scatter in the VHCF life data that reveal number of cycles to fracture covering three orders of magnitude for an identical stress amplitude, evaluation of the test data is linked to a high degree of uncertainty.

Cyclic plasticity in the first stage of VHCF of DSS is limited to slip bands in the fcc austenite phase. Dislocations are piled up at

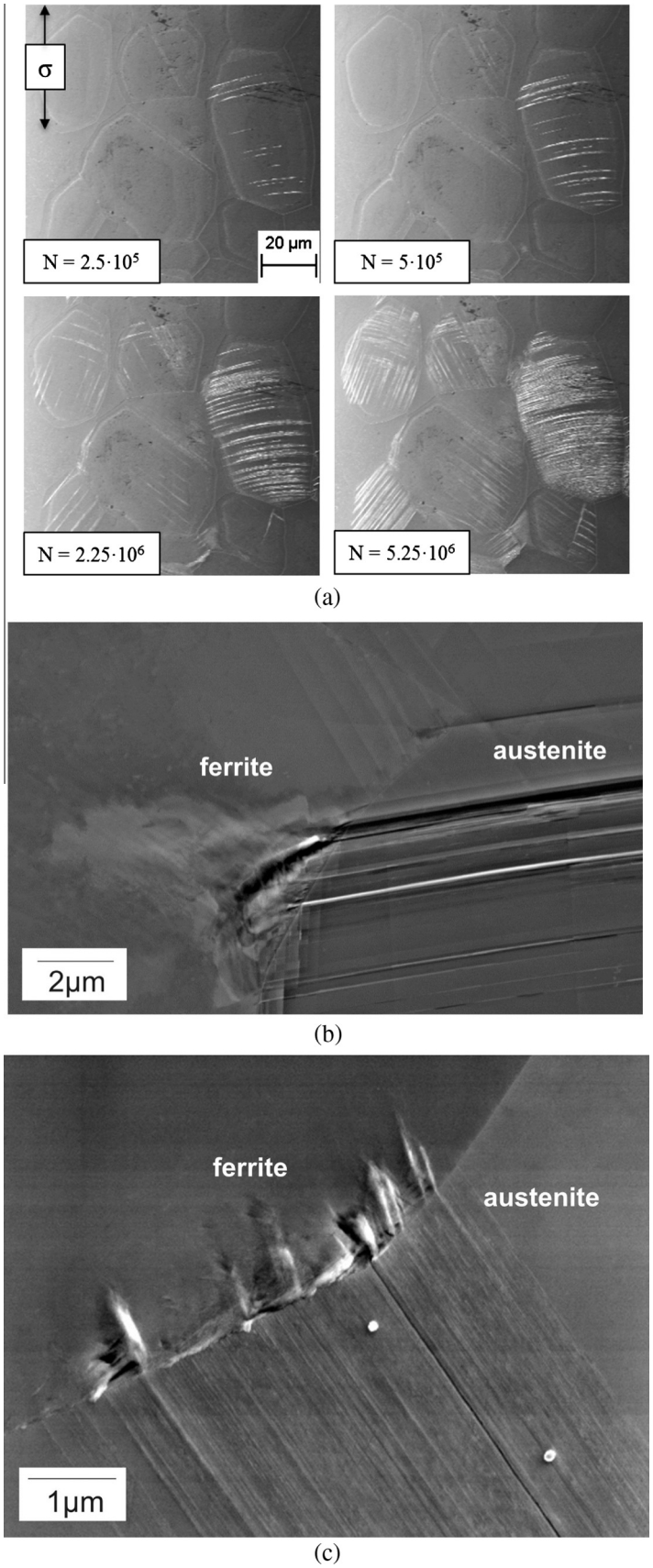

Fig. 10. Fatigue crack initiation during VHCF of DSS (non-embrittled condition): (a) *In-situ* observation of slip band accumulation within the austenite phase, where *N* is the number of cycles, (b) transgranular and (c) intergranular crack initiation at an austenite ferrite phase boundary.

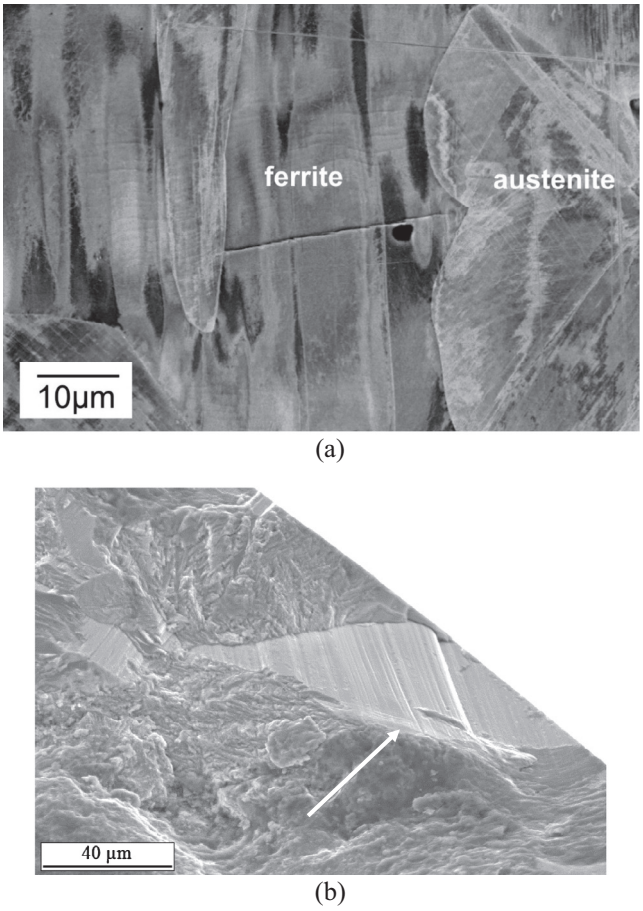

Fig. 11. Micro cleavage (slip-band cracking) during VHCF of fully embrittled specimen: (a) cracked surface slip band in a run-out specimen ($\Delta\sigma/2 = 360$ MPa, $N_f = 10^9$) and (b) micro-cleavage facets (see arrow) in ferrite grains close to the crack initiation site ($\Delta\sigma/2 = 360$ MPa, $N_f = 1.5 \cdot 10^6$).

the austenite ferrite phase boundaries as it is shown in the TEM micrograph in Fig. 9 taken from a run-out specimen.

Work hardening at the operated slip bands causes the activation of new bands, i.e., the density of slip bands within the austenite grains increases with increasing number of load cycles. This behaviour is demonstrated in Fig. 10a, showing a series of surface micrographs that were taken during *in-situ* ultrasonic loading within the SEM (cf. [17]). Of course, plastic deformation limited to one phase in a two phase materials gives rise to the formation of internal stresses. Of particular significance are the stresses in the vicinity of intersection points between the slip bands and the phase boundary at the surface. As revealed by the example in Fig. 10b, such intersection points may act as initiation sites for transgranular fatigue crack growth into ferrite grains. Depending on the slip band density and the intrinsic phase boundary strength, the intersection points may coalesce forming intergranular crack initiation (Fig. 10c).

As a common feature during VHCF of fully embrittled duplex steel, slip activity in the ferrite grains is very localized and seems to be limited to individual $\{1\,1\,0\}\langle 1\,1\,1\rangle$ type slip systems, eventually leading to micro cleavage. An example is shown in Fig. 11, where Fig. 11a shows a deformation-less slip band crack in a ferrite grain. Such cracks manifest themselves in the fracture surface as quasi-cleavage facets (Fig. 11b).

One of the ferrite slip bands in the fully embrittled fatigued DSS was prepared for APT. According to Section 2, a small section containing the slip bands was lift out and sharpened by FIB milling.

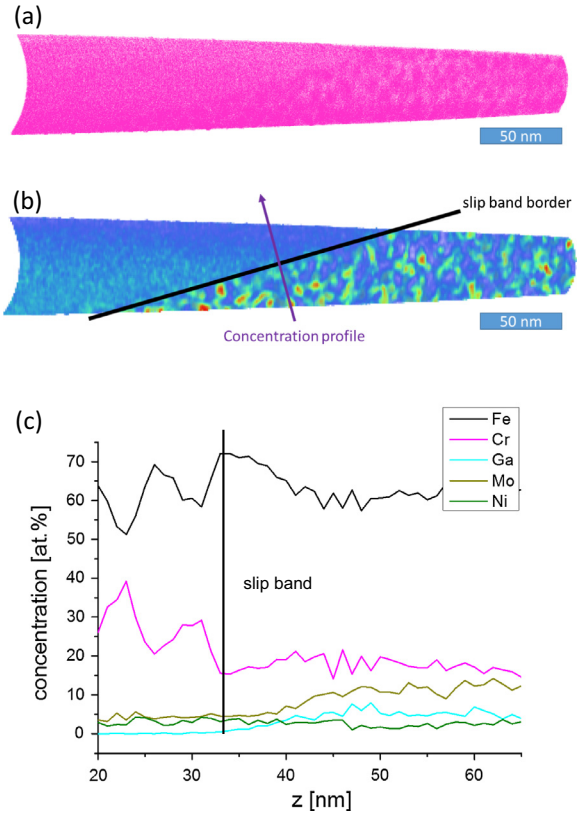

Fig. 12. APT measurement of the Cr ion distribution in VHCF-loaded fully embrittled DSS (run-out specimen, $N = 10^9$, scales are in nm): (a) Cr ion map of a slice through the whole analysed volume, (b) Cr concentration heat map of the same area as in (a), showing a band with α′ dissolution (marked by black line). A concentration profile (c) perpendicular to the slip band demonstrates the difference between the cluster rich area and the slip band.

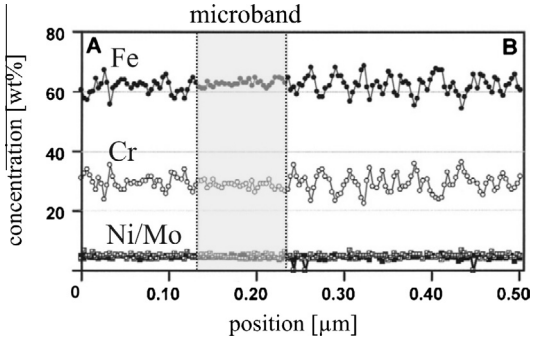

Fig. 13. EDS compositional profile along a line A to B crossing a deformation microband (according to [15]).

Fig. 12 shows a reconstruction of the resulting tip, showing the distribution of Cr ions (Fig. 12a) and the corresponding Cr concentration heat map (Fig. 12b). The Cr enrichments, with diameters of approx. 10 nm, were identified as α′ precipitates that were generated by spinodal decomposition during thermal treatment at 475 °C for 100 h (cf. [22]). In several tips taken form the slip band area, regions were found where the Cr modulation disappeared (cf. region above the black line in Fig. 12a). We conclude that this disappearance coincides with the dislocation activity along the slip bands. It should be added that within the slip band areas, an enrichment in Mo and Ga was found. It is not very probable that the Ga ions cause the partial dissolution of the α′ precipitates, since this was never observed in earlier studies (cf. [23]). However, it

cannot be ruled out that slip bands act as an easy path for Ga ion penetration leading to local damage of the a′ precipitation structure. The more detailed analysis of changes in the micro chemistry in slip bands is subject of ongoing research.

4. Discussion

The fatigue damage behaviour of DSS in the VHCF regime is determined by the spatial arrangement of grain/phase size, crystallographic orientation and the individual strength of the two phases fcc austenite and bcc ferrite and depends strongly on the phase boundary strength against slip transmission. It has been shown that in the case of DSS studied in the present paper, the ferrite phase is the stronger, i.e., planar dislocation arrangements along {1 1 1} slip bands in the fcc austenite are piled up at the respective phase boundaries during fatigue loading. This kind of barrier effect has been correlated quantitatively with the degree of crystallographic misorientation (twist component) between the neighbouring slip systems and simulated by means of a boundary element short crack model in [24,25].

Beside the geometric barrier effect due to the misorientation, slip transmission depends also on the intrinsic barrier strength of the alloy's phase and grain boundaries as well as on the critical shear stress (cyclic friction stress τ_{fr}) to activate dislocation motion at the respective slip bands in the adjacent grain. In the case of DSS, τ_{fr} can be altered by nitrogen alloying and by the spinodal decomposition of the bcc ferrite phase, respectively. Due to the enrichment of nitrogen within the austenite phase, nitrogen alloying contributes mainly to the austenite strength by preventing an easy slip band formation. This results in a substantially higher fatigue strength of N-alloyed super duplex steel, cf. [2,10].

The formation of small α′ precipitates by spinodal decomposition was considered as an alternative way of precipitation strengthening. Obviously, the nm-scale precipitates can be sheared by dislocations. However, the increase in strength is linked to a loss in ductility and therefore, the spinodal decomposition has been termed "475 °C embrittlement". While during quasi-static tension and low-cycle fatigue (LCF), the effect is detrimental, in HCF strengthening by spinodal decomposition seems to have a beneficial effect on fatigue life. However in VHCF, the strengthening effect became not evident. To understand the interactions between the Cr rich α′ precipitates and local plasticity, APT was applied to slip bands in fully embrittled VHC-loaded DSS specimens revealing that the precipitates (Cr modulation) disappears locally (Fig. 12c). This supports the hypothesis by Herenú et al. [15], who showed a slight smoothening in the Cr concentration within deformation bands (LCF-loaded DSS) with analytical TEM. An example of the respective results is shown in Fig. 13. The disappearance of the Cr modulation within the slip band area in LCF was confirmed by the APT analysis of VHCF slip bands, where modulations in the Cr concentration were shown to disappear due to the dissolution of the α′ phase. Obviously, cyclic plasticity in VHCF cause a local softening within the operated slip systems.

5. Conclusions

The very-high-cycle-fatigue (VHCF) behaviour of duplex stainless steels (DSS) can be optimized by adapting the individual strengths of the two phases, austenite and ferrite, respectively. While the softer austenite carries incident cyclic plasticity, the ongoing fatigue damage process is governed by microstructural obstacles, i.e., the phase boundaries between the austenite and the ferrite grains. The barrier strength of these obstacles depends on the degree of coplanarity between operating slip systems and the strength of the ferrite grains. Spinodal decomposition of the ferrite due to thermal treatment at 475 °C results in a pronounced strength increase of the ferrite grains, and hence causes an increase in HCF strength, which, however, was not confirmed to the VHCF regime. Investigations of the slip band chemistry by atom probe tomography revealed that cyclic plasticity coincides with a dissolution of the strengthening precipitates.

Acknowledgments

The financial support by Deutsche Forschungsgemeinschaft DFG in the framework of the priority program SPP1466 *Infinite Life for Cyclically Loaded High Performance Materials* is gratefully acknowledged. Furthermore, one of the authors (UK) wants to express his gratitude to Prof. Krystyna Stiller, Prof. Mats Halvarsson and Dr. Magnus Hörnqvist Colliander for providing him the possibility to stay as affiliated professor at Chalmers University of Technology and to use the facilities of the Division of Materials Microstructure.

References

[1] Alvarez-Armas I, Degallaix-Moreuil S, editors. Duplex stainless steels. London: ISTE; 2009.
[2] Söker M, Schönfeld O, Dönges B, Giertler A, Krupp U. Ermüdungsverhalten von Duplex-Stählen unter Atmosphäreneinfluss. In: Borsutzki M, Moninger G, editors. Proc Werkstoffprüfung Bad Neuenahr. p. 55–61.
[3] Krupp U, Alvarez-Armas I. Short fatigue crack propagation during low-cycle, high cycle and very-high-cycle fatigue of duplex steel – a unified approach. Int J Fatigue 2014;65:78.
[4] Krupp U, Giertler A, Söker M, Fu H, Dönges B, Christ H-J, et al. The behavior of short fatigue cracks during very high cycle fatigue of duplex stainless steel. Eng Fract Mech 2015;145:197–209.
[5] Zhai T, Wilkinson AJ, Martin JW. A crystallographic mechanism for fatigue crack propagation through grain boundaries. Acta Mater 2000;48:4917–27.
[6] Marx M, Schäf W, Vehoff H. Interaction of short cracks with the local microstructure. Proc Eng 2010;2:163–71.
[7] Marinelli M-C, El Bartali A, Signorell JW, Evrard P, Aubin V, Alvarez-Armas I, et al. Activated slip systems and microcrack path in LCF of a duplex stainless steel. Mater Sci Eng A 2009;509:81–8.
[8] Mercier D, Zambaldi C, Bieler TR. A Matlab toolbox to analyze slip transfer through grain boundaries. Proc. 17th international conference on textures of materials (ICOTOM 17), Dresden, Germany 2014, IOP conference series: materials science and engineering, vol. 82. p. 1.
[9] Kübbeler M, Roth I, Krupp U, Fritzen C-P, Christ H-J. Simulation of stage I-crack growth using a hybrid boundary element technique. Eng Fract Mech 2011;78:462.
[10] Lillbacka R, Chai G, Ekh M, Liu P, Johnson E, Runesson K. Cyclic stress–strain behavior and load sharing in duplex stainless steels: aspects of modeling and experiments. Acta Mater 2007;55:5359.
[11] Sahu JK, Krupp U, Ghosh RN, Christ H-J. Effect of 475 C embrittlement on the mechanical properties of duplex stainless steel. Mater Sci Eng 2009;A508:1.
[12] Nilsson JO. Overview: super duplex stainless steels. Mater Sci Technol 1992;8:685.
[13] Lagneborg RG. Deformation in an iron-30% chromium steel aged at 475 °C. Acta Metall 1967;15:1737.
[14] Park KH, Lasalle JC, Schwartz LH. The low cycle fatigue behavior of spinodally decomposed Fe–26Cr–1Mo alloys. Acta Metall 1985;33:205.
[15] Herenú S, Sennour M, Balbi M, Alvarez-Armas I, Thorel A, Armas AF. Influence of dislocation glide on the spinodal decomposition of fatigued duplex stainless steels. Mater Sci Eng A 2011;528:7636.
[16] Kolmorgen R, Henkel S, Biermann H. Thermo mechanical fatigue behaviour of a duplex stainless steel in the temperature range of 350 °C to 600 °C. In: Proc Int Conf on Low Cycle Fatigue LCF 7 2013, Aachen, Germany.
[17] Söker M, Galster M, Dönges B, Krupp U. Ultrasonic fatigue testing in the scanning electron microscope. Mater Test 2016;58:1.
[18] Miller MK, Forbes RG. Atom-probe tomography: the local electrode atom probe. New York Heidelberg: Springer; 2014.
[19] Wackermann K. Einfluss einer zyklischen Belastung auf die Versprödungskinetik von Legierungen am Beispiel der 475 °C-Versprödung von Duplexstahl und der dynamischen Versprödung einer Nickelbasislegierung, Dissertation Univ. Siegen; 2015.
[20] Krupp U, Giertler A, Marinelli MC, Knobbe H, Christ HJ, Köster P, et al. Efficiency of grain and phase boundaries as microstructural barriers during HCF and VHCF loading of austenitic-ferritic duplex steel. In: Proc 5th Int Conf VHCF, Berlin; 2011. p. 127.
[21] Krupp U, Knobbe H, Christ HJ, Köster P, Fritzen CP. The significance of microstructural barriers during fatigue of a duplex steel in the high- and very-high-cycle-fatigue (HCF/VHCF) regime. Int J Fatigue 2010;32:914–20.
[22] Pettersson N, Wessman S, Thuvander M, Hedström P, Odqvist J, Pettersson RFA, et al. Nanostructure evolution and mechanical property changes during

aging of a super duplex stainless steel at 300 °C. Mater Sci Eng A 2015;647:241.
[23] Bjurman M, Thuvander M, Liu F, Efsing P. Phase separation study of in-service thermally aged cast stainless steel – atom probe tomography. In: Proc 17th Int Conf Environmental Degradation of Materials in Nuclear Power Systems – water Reactors, Ottawa, Canada; 2015.
[24] Künkler B, Schick A, Fritzen C-P, Floer W, Krupp U, Christ H-J. Simulation of microstructurally controlled short crack propagation. Steel Res 2003;74:514–8.
[25] Marinelli MC, Krupp U, Kübbeler M, Hereñú S, Alvarez-Armas I. The effect of the embrittlement on the fatigue limit and crack propagation in a duplex stainless steel during high cycle fatigue. Eng Fract Mech 2013;110:421–9.